

## Determination of finite strain in bedding surfaces using sedimentary structures and trace fossils: a comparison of techniques

JOHN W. F. WALDRON

Geology Department, Saint Mary's University, Halifax, Nova Scotia, Canada B3H 3C3

(Received 16 June 1987; accepted in revised form 7 December 1987)

**Abstract**—Determination of the two-dimensional finite strain in turbidite bedding surfaces is important in both structural and sedimentological investigations of deformed sediments. The Meguma Group of Nova Scotia is one such sequence, in which the directional distribution of paleocurrent markers has been modified by strain. Previous strain determinations have used sand volcanoes as strain markers, which do not deform homogeneously with their matrix and, hence, may underestimate the true strain ratio. Intraclasts and concretions also suffer inhomogeneous deformation and are of limited use as strain markers. Hexagonal trace fossil networks can provide more reliable strain estimates but are rare. Widths of burrows exposed on bedding surfaces provide a new, straightforward means of measuring strain. Each burrow is represented by a pair of parallel lines. The separation of the lines is proportional to the burrow width, and their direction represents burrow orientation. The lines are tangential to the strain ellipse, which can be discerned despite initial scatter in burrow widths.

### INTRODUCTION

A VARIETY of techniques exist for the determination of finite strain in two dimensions in deformed sedimentary rocks. Of particular importance are determinations of the strain ellipse in bedding surfaces. Estimates of bedding-surface strain are necessary for the restoration of paleocurrent distributions to their original shape, and may provide important evidence of the timing of distortion, cleavage development, and folding. This paper compares the practical usefulness of several established techniques for the assessment of the two-dimensional finite strain in turbidite bedding surfaces, emphasizing the difficulty of obtaining suitably large samples of markers with known initial shape and homogeneous deformation. A new method using trace fossils is described that avoids many of the difficulties of existing techniques.

The Cambro-Ordovician Meguma Group of southwest Nova Scotia, in the Canadian Appalachians (Fig. 1), is a thick sequence of interbedded psammities and slates that were probably first deformed in the Middle Devonian Acadian Orogeny. The Group is conventionally divided into two formations. The lower, Goldenville Formation, consists mainly of medium to very thickly bedded metamorphosed sandstones with subordinate interbedded slates; the overlying Halifax Formation is mainly slate but contains subordinate, generally thinly bedded sandstones. Both formations are folded into upright to steeply inclined, close to tight, sub-horizontal map-scale folds with axes that trend roughly NE-SW. A penetrative, steeply dipping axial-planar slaty cleavage is developed in the fine-grained beds and a spaced pressure-solution cleavage is present in some psammities. Mesoscopic folds are generally rare; primary features of the sediments are best observed on the approximately homoclinal sections on the limbs of the

major folds. The sandstones in both formations are interpreted as turbidites (Phinney 1961, Stow *et al.* 1984). Campbell (1966) and Schenk (1970) measured the orientations of flutes and grooves, restoring them to horizontal by simple rotation about the strike. Harris (1971), recognizing the need to remove the effects of tectonic strain before interpreting paleocurrent patterns, used the shape of sand volcanoes on bedding surfaces to estimate the strain ratio ( $R_s$ ) in bedding surfaces. Studies of the structural evolution of the Meguma Group (Henderson *et al.* 1986) have used the same method of strain determination. They found little difference between the strains indicated by sand volcanoes on fold hinges and fold limbs, and on the basis of this and other observations postulated that the majority of cleavage development took place prior to folding. However, Henderson *et al.* (1986) also noted a

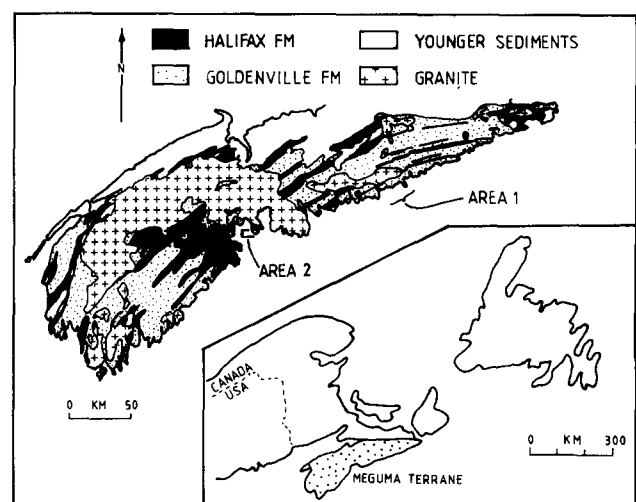


Fig. 1. Geological map of southern mainland Nova Scotia showing extent of Halifax and Goldenville Formations and locations of study areas.

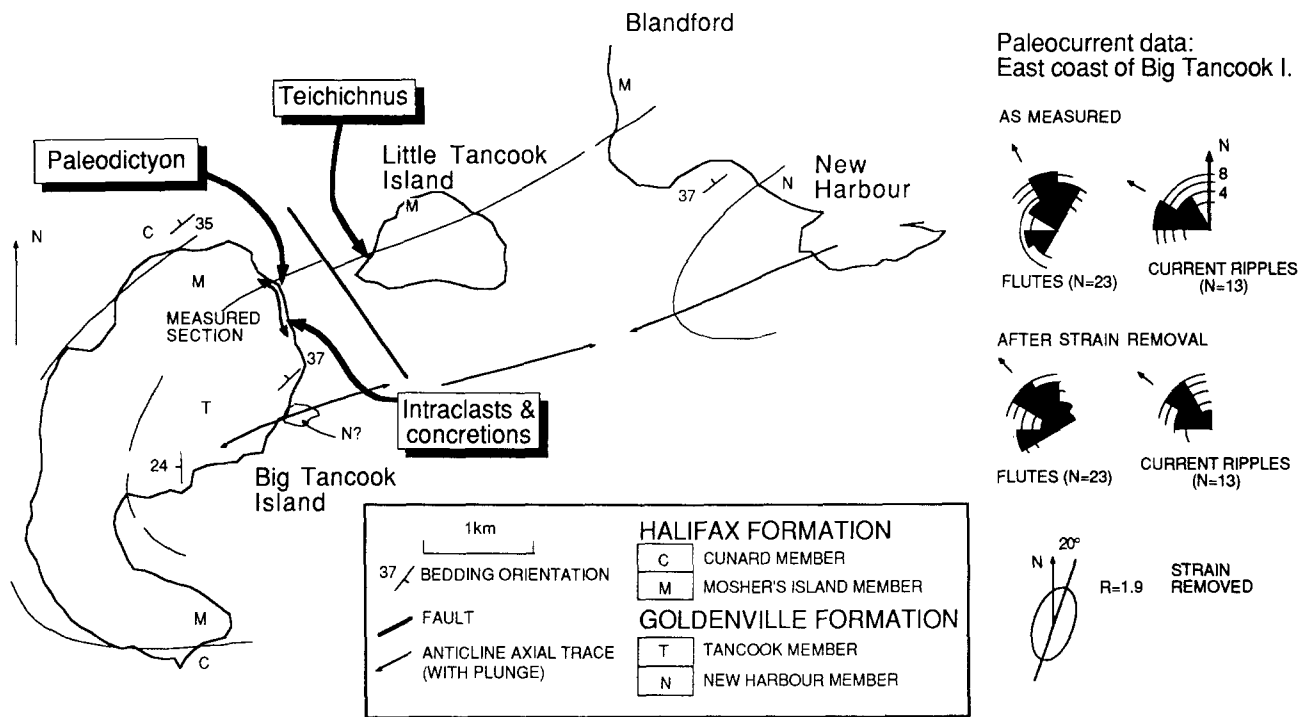


Fig. 2. Schematic geological map of area 2 showing location of outcrops used for strain determination and measured section from which paleocurrent data were collected. Circular histograms at right show paleocurrents deduced from flutes and ripples before and after strain removal. Lower diagrams show results of strain removal. Flutes and ripple crest orientations were re-orientated using strain estimated from *Paleodictyon* networks; diagrams for ripples show current directions deduced from internal cross-lamination, after unstraining of ripple crest orientations.

divergence of the bedding–cleavage intersection lineation around sand volcanoes, suggesting that the volcanoes did not deform homogeneously with their matrix.

Following two sedimentological investigations by the author (Waldron & Jensen 1985, Waldron 1987), attempts were made to improve upon previous methods of strain determination, in order to obtain a more accurate picture of the shape of the paleocurrent distribution. Sedimentological results have been and will be presented elsewhere; the remainder of this paper compares the effectiveness of the various types of strain determination.

### STRAIN MARKERS

Assumptions about the initial shape and behaviour during deformation of strain markers cannot be directly justified; hence, it is desirable to use two or more independent types of strain marker for strain determination in any given area. The following paragraphs describe the use of a variety of strain markers available in two study areas (Fig. 1). Area 1 is located on the Eastern Shore of Nova Scotia, in the Goldenville Formation. Area 2 is located on the South Shore of Nova Scotia, at the transition between the Goldenville and overlying Halifax Formation (Fig. 2).

#### *Sand volcanoes*

Most previous strain determinations in the Meguma sediments have been based on the shapes of sand vol-

canoes (Fig. 3a), i.e. mounds produced by syndimentary dewatering of rapidly deposited massive sandstones (Pickerill & Harris 1979). Sand volcanoes may completely cover the top surfaces of such beds, which also show internal evidence of dewatering such as pillar structures, dish structures (Lowe & Lopiccolo 1974), sheet structures (Laird 1970) and convolute lamination. Sand volcanoes are unusually common in the Goldenville Formation, but are also recorded in other turbidite successions (e.g. Stringer & Treagus 1980). Most volcanoes show a central vent-like depression, and in ideal outcrops a 'feeder' pillar structure of coarser, better sorted sandstone may be seen, but Henderson *et al.* (1986) describe volcanoes occurring also in linear arrays above sheet structures. Harris (1971) reported an aspect ratio of 1.5 for sand volcanoes within area 1, whereas Henderson *et al.* (1986) obtained a wide scatter of ratios concentrated between 1.8 and 2.6 (extreme values 1.1 to 3.3) from 827 sand volcanoes in the coastal area east of area 1.

Sand volcanoes are not ideal as strain markers in the Meguma sediments for a number of reasons. Firstly, volcanoes are difficult to measure objectively; only on exceptional beds does erosion show perfectly bed-parallel cross-sections with sharply defined margins (e.g. Henderson *et al.* 1986, fig. 3B). Secondly, because dewatering may have occurred very soon after deposition of a turbidite sand layer, while waning currents were still flowing, the volcanoes may not have had perfectly circular initial shapes; the common central location of the vent indicates that this is not a serious problem. Thirdly, divergence of the intersection line-

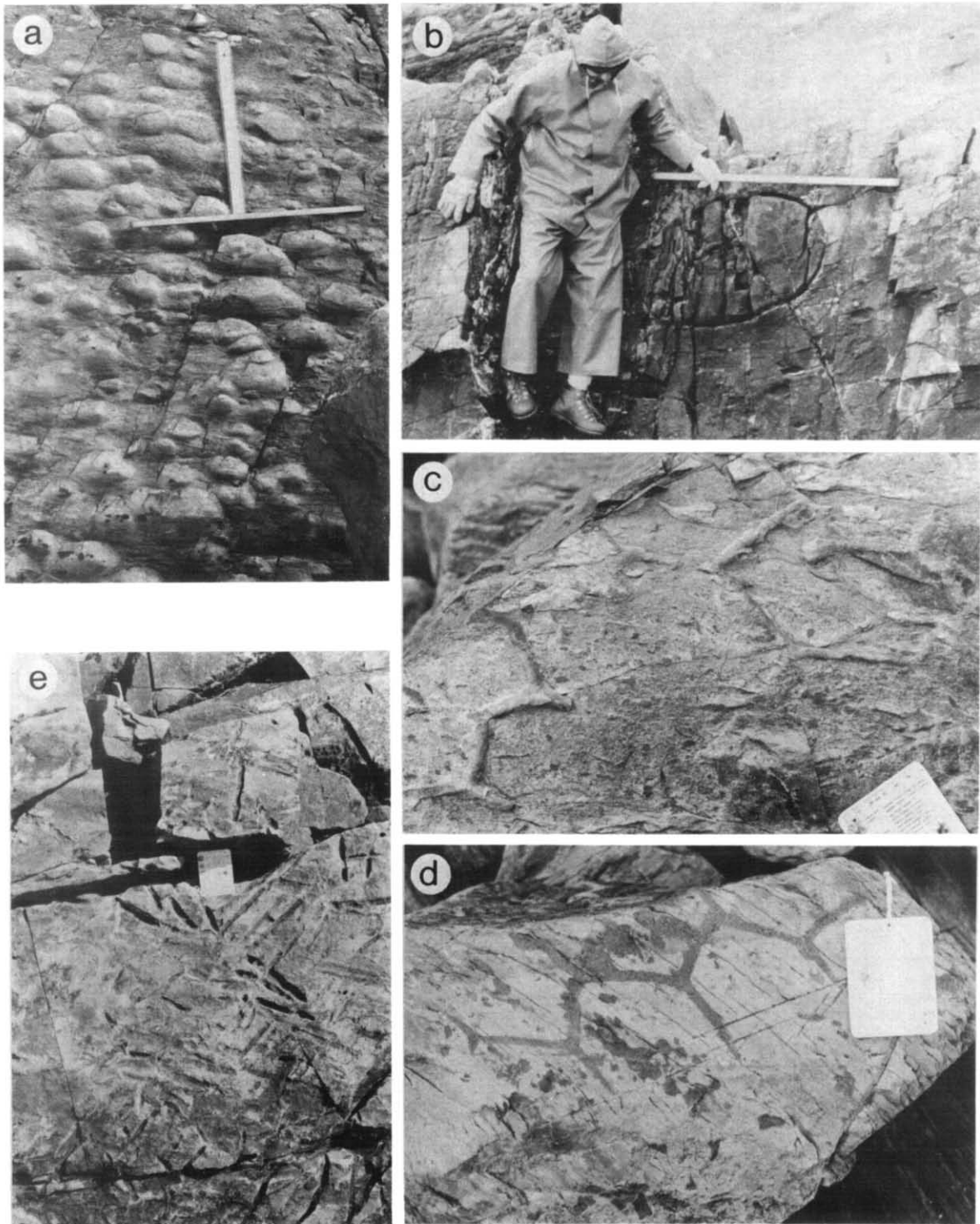


Fig. 3. Field photographs of sedimentary structures used for strain determination. (a) Sand volcanoes; horizontal ruler is 1 m long. (b) Large carbonate concretion in massive sandstone bed (scale 1 m). (c) *Paleodictyon* burrow network exposed in relief on base of sandstone bed. Card is 6.5 cm wide. (d) *Paleodictyon* burrow network preserved embedded in top of slate interval that formerly underlay sandstone bed. Card is 6.5 cm wide. (e) *Teichichnus* burrows on bedding surface. Card is 6.5 cm wide.



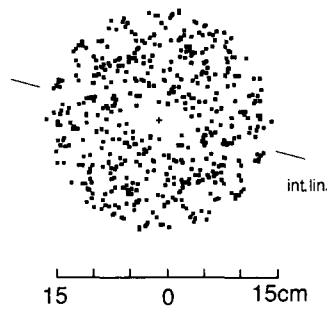


Fig. 4. Fry plot of sand volcano centres obtained from bed shown in Fig. 3(a) in area 1. Horizontal in diagram represents line of zero pitch (strike) in bedding surface.

ation around volcanoes noted by Henderson *et al.* (1986) implies that the coarser sand volcanoes behave more competently than their matrix and may underestimate the total strain. More seriously, the volcanoes may have rotated relative to their matrix; bed-parallel cross-sections are not therefore representative of the bulk bedding-plane strain.

Waldron & Jensen (1985) used a Fry plot (Fry 1979) based on distances between volcano centres, thus avoiding these potential problems. Figure 4 shows a Fry plot based on the distribution of 65 sand volcanoes on a single bedding surface in area 1. The plot does not tightly constrain the shape of the strain ellipse, but suggests a strain ratio in the range 2.0–2.5, somewhat larger than Harris' (1971) estimate of 1.5, though consistent with the strain ratios obtained by Henderson *et al.* (1986) farther east. The usefulness of Fry's method is limited by the difficulty of finding suitable surfaces with adequate numbers of exposed volcanoes; Crespi (1986) has recommended that 200–800 points be used, depending on the strength of anticlustering. Furthermore, some surfaces do not produce anticlustered plots, presumably because the volcanoes did not have the required statistically uniform initial distribution; Ramsay & Huber (1983) emphasize that a completely random, or Poisson, distribution of points will not produce an anticlustered plot. The method is also vulnerable to anisotropies in the initial distribution of volcanoes, such as might occur if volcanoes are located over sheet-like dewatering structures whose orientations are controlled by a primary sedimentary fabric in the sandstones (Laird 1970).

#### *Intraclasts and concretions*

Intraclasts of fine-grained interturbidite sediments are common in turbidite sandstones, and are usable as strain markers when they have well rounded, elliptical outlines visible on bedding surfaces. Because the intraclasts show variation in their shapes and orientations, an  $R_f/\phi$  plot is appropriate; Fig. 5 shows results from a single bed in area 2. The harmonic mean value of  $R_f$  is 2.0. Comparison of Fig. 5 with standard curves of Ramsay & Huber (1983) indicates a tectonic strain ratio ( $R_t$ ) of between 2.0 and 2.5. Their approximate formulae based on the minimum and maximum value of  $R_f$  yields an estimate of 2.2.

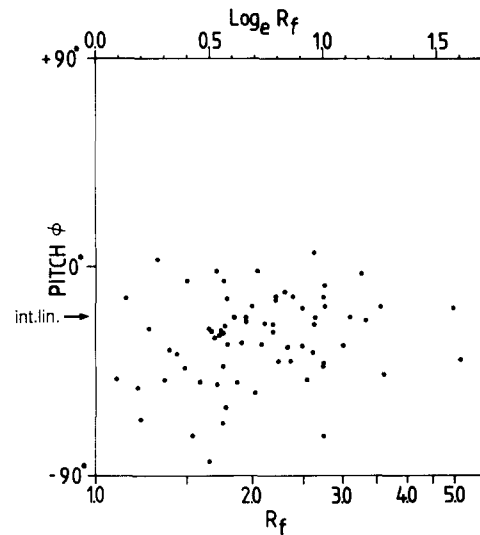


Fig. 5.  $R_f/\phi$  plot representing 67 intraclasts in bedding surface, area 2.

The initial distribution of intraclast orientations is likely to have been controlled by sedimentary processes. Clasts in turbidites tend to settle with the horizontal projection of their long axes orientated parallel to flow (Walker 1984). In area 2 the majority of paleoflow directions were probably towards the NW, roughly perpendicular to the extension axis implied by Fig. 5; preferred initial orientation of long axes in this direction would lead to an underestimate of the true tectonic strain. A slight asymmetry of the scatter in Fig. 5 perhaps also reflects an initial preferred orientation. Furthermore, the intraclasts are likely to have behaved incompetently relative to their sandstone matrix during deformation. The strain estimate obtained from intraclasts must therefore be regarded as approximate.

Thick homogeneous sandstone beds in area 2 sometimes contain large, ellipsoidal carbonate concretions (Fig. 3b). Although these are not present in sufficient numbers for the use of the  $R_f/\phi$  technique, they may also provide rough estimates of the strain, assuming their bed-parallel cross-sections were initially circular. The typical large concretion in Fig. 3(b), located close to the intraclasts described above, has an aspect ratio of 1.46. However, divergence of the intersection lineation at the edges of the concretion suggests that it behaved competently and therefore underestimates the strain. The estimate could be further invalidated if the concretion had an initially elliptical shape due perhaps to a permeability anisotropy existing in the sand during cementation.

#### *Paleodictyon-type trace fossils*

Hexagonal bed-parallel burrow networks of *Paleodictyon* type occur in the *Nereites* ichnofacies (Seilacher 1967), typical of turbidites. The burrows are believed to have been constructed just below the sediment–water interface, but were exhumed during the erosive phase of a turbidity current, and are preserved as sand-filled sole marks (Fig. 3c & d). Their general location, composition

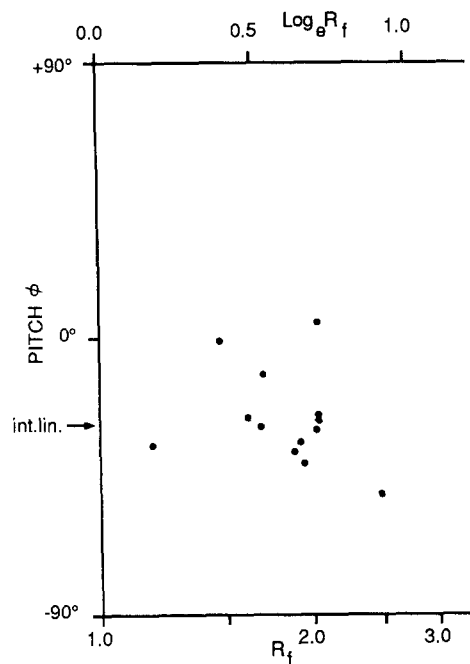


Fig. 6.  $R_f/\phi$  plot representing 12 three-way intersections in *Paleodictyon* burrow networks, area 2.

and dimensions are in fact closely comparable to those of paleocurrent indicators such as flutes and grooves, making them potentially almost ideal as strain markers.

Burrows have been recorded from a single *in situ* bedding surface in area 2, and from a number of loose boulders. (The bedding–cleavage intersection lineation was used as a constant reference direction in making measurements from loose blocks.) For strain determination, it is necessary to assume that the networks were constructed of regular hexagons with  $120^\circ$  angles; each

three-way intersection then provides sufficient information for a strain determination. This assumption is at least approximately true for many undeformed examples of *Paleodictyon*. However Chamberlain (1971) and Seilacher (1977) studied the details of *Paleodictyon* burrows and showed that the organism's behaviour did not show perfect hexagonal symmetry; the network was constructed in rows as shown in Fig. 7(a). Thus some departure from the assumed initial symmetry of burrows might be expected. Ragan & Sheridan (1972) describe strain determination from trilete glass shards, geometrically equivalent to the burrow intersections, using the Mohr circle construction. Sanderson (1977a) gave an equivalent algebraic method for arbitrarily orientated rosettes of lines, which was used in this study. The results of measurements from a total of 12 well-preserved intersections on two separate surfaces are shown in Fig. 6. Interpretation of Fig. 6 is limited by the small number of measurements that were possible and the considerable scatter of  $R_f$  and  $\phi$  values, but suggests a strain ratio of about 1.9.

#### *Teichichnus*-type trace fossils

The upper part of the Goldenville Formation in area 2 contains numerous sheet-like spreite burrows of *Teichichnus* type; their geometry is shown schematically in Fig. 7(b). Viewed on weathered bedding surfaces these burrows produce slot-like depressions as shown in Fig. 3(e). If the burrows had originally random orientations, and behaved as passive line markers during deformation, their distribution with direction should now show concentration parallel to the extension direction. Figure 8(a) shows plots of concentration against direc-

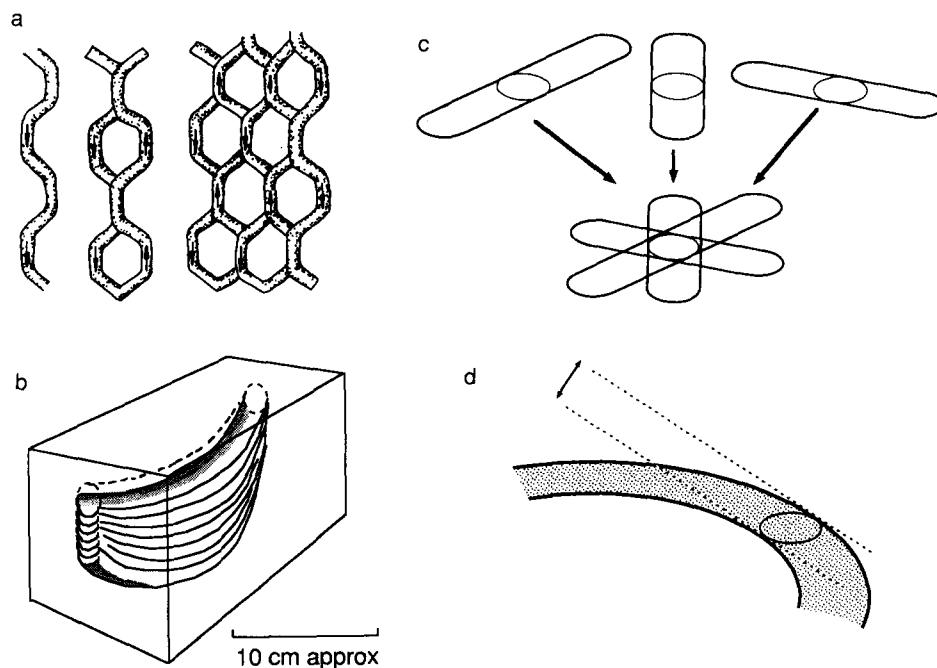


Fig. 7. Trace fossil geometry and strain measurement. (a) Mode of construction of *Paleodictyon* networks, after Chamberlain (1971). (b) Geometry of *Teichichnus* spreiten. (c) Principle of tangential plot for *Teichichnus* burrow widths. If ideal burrows have uniform widths then burrow sides are tangents to strain ellipse; burrows can be superimposed, defining the inscribed ellipse. (d) Measurement method for widths of curved burrows or trails.

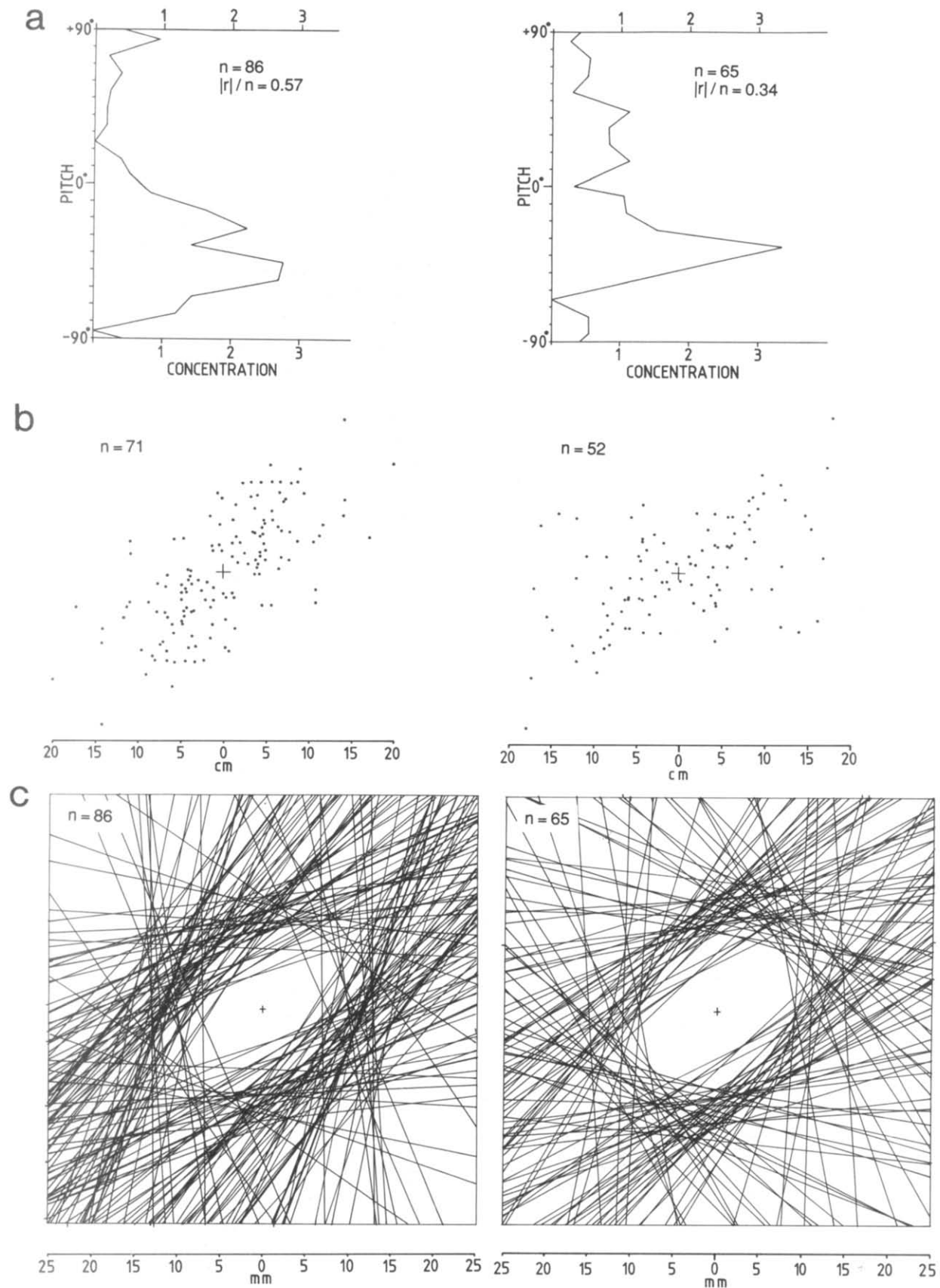


Fig. 8. (a) Plots of concentration of *Teichichnus* burrows vs pitch in bedding surface shown in Fig. 3(e). Plots are for two arbitrary sub-areas of surface (separated by trace of a major joint). (b) Plots showing distribution of *Teichichnus* lengths vs pitch. Horizontal in plot represents the strike (zero pitch). Each measured burrow length is represented by two points symmetrically on either side of origin. Plots are for same two arbitrary sub-areas as in (a). Sample sizes are smaller because burrows intersecting margins of sub-areas were excluded. (c) Tangential plots of burrow widths, constructed as in Fig. 7(c). Horizontal edge of diagram represents strike direction.

tion for two arbitrary sub-areas on a single bedding surface, and shows values of the normalized resultant vector magnitude ( $|r|/n$ ), which may be used to estimate the apparent strain ratio  $R$  in the method of Sanderson (1977b). The calculated values of  $|r|/n$  (0.57 and 0.34) imply strain ratios of 3.8 and 2.1, respectively, with no overlap of 90% confidence limits. The directions of maximum concentration are also different in the two sub-areas. Either strain was dramatically inhomogeneous or the initial distribution was non-random. Closer examination of the burrows reveals clusters of similarly orientated burrows at several locations in the bedding surface. Thus the initial assumption of random burrow orientation is almost certainly false.

Despite the non-random distribution of burrow orientations, the lengths of *Teichichnus* burrows before deformation might be expected to vary independently of direction. Figure 8(b) shows the variation with pitch of burrow lengths for the same sub-areas as Fig. 8(a). Each burrow is plotted as two symmetrically opposite points to aid visualization of the shape of the resulting cluster. One sub-area shows a convincingly elliptical cluster, but the other shows maximum concentration in an elongated spindle-shaped area of the plot, demonstrating that the initial distribution of lengths was also non-uniform. The organism may have produced longer burrows when excavating in its preferred direction.

Widths of burrows were also measured to the nearest millimetre. Burrow sides in general suffered non-zero shear strain; thus the widths measured in the deformed state do not in general represent lines that were true burrow-widths before deformation, and a plot such as Fig. 8(b) cannot be used. However, burrow sides can be regarded as tangents to a strain ellipse as shown in Fig. 7(c). This suggests a new method of plotting shown in Fig. 8(c), in which each measured burrow is represented by a pair of parallel lines symmetrically placed on opposite sides of the origin. The perpendicular distance of each line from the origin represents the width of the burrow and its direction represents the pitch of the burrow in the bedding surface. Figure 8(c) shows plots for the same two sub-areas as Fig. 8(a) & (b). In both cases the burrow sides outline a well-defined ellipse. Estimation of the strain ratio and orientation is best achieved by superimposing concentric sets of standard ellipses drawn for various aspect ratios over the plots shown in Fig. 8(c), so as to best fit the elliptical zone of most densely clustered lines. In both plots the strain ratio is estimated at 1.7. (The intersection lineation is not clearly measurable on the bedding surface that displays the fossils. Nearby measurements indicate that it is at least approximately parallel to the long axes of the ellipses.)

The clear and consistent results indicate that burrow widths were initially statistically uniform and were little influenced by burrow orientation. Presumably burrow width was controlled only by the size of the burrowing organism, whereas the length and orientation of the burrow were influenced by its behaviour. Some strain inhomogeneity might be expected if the laminated sand

of the burrow fills were more or less competent than the surrounding massive sands, but the competence contrast would presumably be much less than that of the fine-grained intraclasts or the coarse-grained sand volcanoes.

*Teichichnus* burrows are unusually abundant in parts of area 2, but the method using burrow widths can easily be applied to almost any type of burrow visible on bedding surfaces. For burrows that are curved, widths must be measured between parallel tangents to the burrow sides as shown in Fig. 8(d). Most Phanerozoic turbidite sequences include beds with meandering, parallel-sided trails preserved as sole marks. Geometrically equivalent burrows are abundant in shallow marine and non-marine sediments also. This method of strain determination should therefore be widely applicable in deformed sedimentary rocks.

### Discussion

The various techniques of strain determination do not give identical results even within the same area. This is probably mainly due to violations of the assumptions implicit in the methods, but the variations may also reflect inhomogeneities in the regional strain, especially in area 2, which is close to a culmination point on a mapped fold (Fig. 2). However, the variations in strain within area 2 are not of sufficient magnitude to seriously disturb the paleocurrent patterns. Figure 2 shows the measured paleocurrents derived from flutes and ripple crest orientations after simple rotation to horizontal about the strike and after removal of the estimated strain. The apparent divergence in current direction, attributed in part to sedimentary processes in an earlier report (Waldron 1987), almost disappears when the flutes and ripple-crests are re-orientated, and must therefore be regarded as a product of tectonic strain.

### CONCLUSIONS

No single method of strain determination is entirely reliable; because of the assumptions involved, at least two independent methods should be used. Trace fossils can provide abundant, rapidly measurable strain markers in many sequences. Widths of burrows are more likely to have an initially uniform distribution than burrow lengths and orientations, which may be influenced by directional behaviour of the burrowing organisms. Because they are often composed of material closely similar in composition and texture to their matrix, burrows are likely to deform approximately homogeneously. In the Meguma Group of Nova Scotia, some previous strain estimates based on the shapes of sand volcanoes may significantly underestimate the strain. In area 1 the strain ratio in bedding surfaces was probably over 2.0, while in area 2 the strain ratio varied between 1.7 and 2.0.

*Acknowledgements*—This study was supported by the Geological Survey of Canada under the Canada–Nova Scotia Mineral develop-



ment agreement, through Supply and Services Canada Contract 23233-6-0052/01-ST with Saint Mary's University. Preparation of the paper was also supported by NSERC Operating Grant A8508. I am grateful to D. J. Sanderson and two anonymous reviewers for helpful comments, to R. K. Pickerill and D. Fillion for advice on trace fossils, and to T. O. Wright, J. R. Henderson, F. W. Chandler and J. Greenough for useful discussions.

## REFERENCES

- Campbell, F. H. A. 1966. Paleocurrents and sedimentation of part of the Meguma Group (Lower Paleozoic) of Nova Scotia, Canada. Unpublished M.Sc. thesis, Dalhousie University, Halifax, Canada.
- Chamberlain, C. K. 1971. Morphology of trace fossils from the Ouachita Mountains, southeastern Oklahoma. *J. Paleontol.* **45**, 212–246.
- Crespi, J. M. 1986. Some guidelines for the practical application of Fry's method of strain analysis. *J. Struct. Geol.* **8**, 799–808.
- Fry, N. 1979. Random point distributions and strain measurement in rocks. *Tectonophysics* **60**, 89–105.
- Harris, I. M. 1971. Geology of the Goldenville Formation, Taylor Head, Nova Scotia. Unpublished Ph.D. thesis, Edinburgh University.
- Henderson, J. R., Wright, T. O. & Henderson, M. N. 1986. A history of cleavage and folding: an example from the Goldenville Formation of Nova Scotia. *Bull. geol. Soc. Am.* **97**, 1354–1366.
- Laird, M. G. 1970. Vertical sheet structures—a new indicator of sedimentary fabric. *J. sedim. Petrol.* **70**, 428–434.
- Lowe, D. R. & LoPiccolo, R. D. 1974. The characteristics and origin of dish and pillar structures. *J. sedim. Petrol.* **44**, 484–501.
- Phinney, W. C. 1961. Possible turbidity current deposit in Nova Scotia. *Bull. geol. Soc. Am.* **72**, 1453–1454.
- Pickerill, R. K. & Harris, I. M. 1979. A reinterpretation of *Astropolithon hindii* Dawson 1878. *J. sedim. Petrol.* **49**, 1029–1036.
- Ragan, D. M. & Sheridan, M. F. 1972. Compaction of the Bishop Tuff, California. *Bull. geol. Soc. Am.* **83**, 95–106.
- Ramsay, J. G. & Huber, M. I. 1983. *The Techniques of Modern Structural Geology. Volume 1: Strain Analysis*. Academic Press, London.
- Sanderson, D. J. 1977a. The algebraic evaluation of two-dimensional strain rosettes. *Math. Geol.* **9**, 483–496.
- Sanderson, D. J. 1977b. The analysis of finite strain using lines with an initial random orientation. *Tectonophysics* **43**, 199–211.
- Schenk, P. E. 1970. Regional variation of the flysch-like Meguna Group (Lower Paleozoic) of Nova Scotia compared to recent sedimentation off the Scotian Shelf. In: *Flysch Sedimentology in North America* (edited by Lajoie, J.). *Spec. Pap. geol. Ass. Can.* **7**, 127–153.
- Seilacher, A. 1967. Bathymetry of trace fossils. *Mar. Geol.* **5**, 413–428.
- Seilacher, A. 1977. Pattern analysis of *Paleodictyon* and related trace fossils. In: *Trace Fossils 2* (edited by Crimes, T. P. & Harper, J. C.). *Geol. J. (Special Issue)* **9**, 289–334.
- Stow, D. A. V., Alam, M. & Piper, D. J. W. 1984. Sedimentology of the Halifax Formation, Nova Scotia: Lower Palaeozoic fine-grained turbidites. In: *Fine Grained Sediments: Deep Water Processes and Facies* (edited by Stow, D. A. V. & Piper, D. J. W.). *Spec. Publ. geol. Soc. Lond.* **15**, 127–144.
- Stringer, P. & Treagus, J. E. 1980. Non axial-planar  $S_1$  cleavage in the Hawick Rocks of the Galloway area, Southern Uplands, Scotland. *J. Struct. Geol.* **2**, 317–331.
- Waldron, J. W. F. 1987. Sedimentology of the Goldenville-Halifax Transition in the Tancook Island area, Nova Scotia. *Geol. Surv. Can. Open File* 1535.
- Waldron, J. W. F. & Jensen, L. R. 1985. Sedimentology of the Goldenville Formation, Eastern Shore, Nova Scotia. *Geol. Surv. Pap. Can.* 85–15.
- Walker, R. G. 1984. Turbidites and associated coarse clastic deposits. In: *Facies Models* (edited by Walker, R. G.). *Geosci. Can. Reprint Ser.* **1**, 91–103.